Journal of Applied Polymer Science

# Facile preparation and separation performances of cellulose nanofibrous membranes

**Faizal Soyekwo, Qiu Gen Zhang, Xiao Chen Lin, Xin Mei Wu, Ai Mei Zhu, Qing Lin Liu**
Department of Chemical and Biochemical Engineering, College of Chemistry & Chemical Engineering, Xiamen University, Xiamen, 361005, China
Correspondence to: Q. G. Zhang (E-mail: qgzhang@xmu.edu.cn) and Q. L. Liu (E-mail: qlliu@xmu.edu.cn)

**ABSTRACT:** Ultrafiltration (UF) is a size selective pressure-driven membrane separation process increasingly required for high efficient water treatment and suspended solids removal in many industrial applications. This study examined the morphology of as-prepared cellulose nanofibers and then utilized the nanofibers dispersion to fabricate nanofibrous nanoporous membranes with potential wide applications in various fields including water treatment. The nanofibers were prepared using a simple and powerful mechanical high intensity ultrasonication following a pre-chemical treatment of α-cellulose. The cellulose nanofibers' morphology, crystallinity, and yield were found to be influenced by pre-chemical treatment. Cellulose nanofibrous membranes were fabricated from cellulose nanofibers dispersion on a porous support. A nanoporous structure with an extensive interconnected network of fine cellulose nanofibers was formed on the support substrate. The resulting membranes exhibited typical and high-efficient UF performances with high water fluxes of up to 2.75 $10^3$ L/$m^2$/h/bar. The membranes also displayed high rejections for ferritin and 10 nm gold nanoparticles with a reactive surface area capable of rapidly decolorizing methylene blue from its aqueous solution. © 2016 Wiley Periodicals, Inc. J. Appl. Polym. Sci. **2016**, *133*, 43544.

**KEYWORDS:** membranes; nanostructured polymers; properties and characterization

Received 13 September 2015; accepted 16 February 2016
**DOI: 10.1002/app.43544**

## INTRODUCTION

The quest for the use of environmentally benign and biocompatible materials has fueled progressive research to be undertaken in the field of natural materials, particularly because these materials are biodegradable and easily obtainable from abundant renewable sources. Cellulose, existing as the most abundant natural polymer and possessing phenomenal mechanical and chemical strength is utilized for making various products such as paper, explosives, plastics, biomaterials, and separation materials.[1,2] With the growing impetus for green chemistry and sustainability sought to be driving the needs of the near future, the development of nanocellulose is a subject of continued interest. This is evidenced by the existing host of publications, setup of collaborative research centers and the establishment of pilot production plants among research scientists.[3] Cellulose nanofibers is an excellent class of nanocellulose materials that exhibits peculiar properties such as high aspect ratio, large surface area, low thermal expansion, and high modulus. These have been exploited in their wide applications in electronic devices, as food thickeners and as a strengthening component in composite materials.[4–6]

Whereas the use of cellulosic fibers in the reinforcement of composites is well reviewed, their use in many filtration applications, specifically in the fabrication of thin film nanofibrous composite membranes with a thin separation layer on a macroporous support is not sufficiently studied. Thin film nanofibrous membranes are considered more efficient than their conventional ultrafiltration (UF) support counterparts produced by phase inversion method. This is because the latter have tight and narrow pore size leading to considerably low flux.[7] Electrospun nanofibers are a feasible approach to fabricate high flux cellulose UF membranes. But the dissolution of cellulose is impractical in aqueous media. It necessitates specialized solvents such as ionic liquids or a combination of special organic solvents systems.[8,9] This would render the dissolution of cellulose in organic solvents for producing electrospun nanofibers as ungreen and environmentally unfriendly. Besides several layers of electrospun fibers are needed to reduce the more open fiber structure resulting in increased thickness of the resultant membranes. Therefore, barrier layer nanocellulose materials that can be produced using the most suitable green approaches and are

Additional Supporting Information may be found in the online version of this article.

able to form highly porous thin films with a low resistance to water permeation are desirable.

Recently, Varanasi *et al.* (2015) developed ultrafiltration (UF) membranes of cellulose nanofibers. Although their preparation method of the cellulose nanofibers is rapid, the dimensions of the produced nanofibers are large and not uniformly distributed, requiring the incorporation of nanoparticles to achieve pore size control of their resultant membranes.[10] Ma *et al.* (2014) used an approach based on the TEMPO oxidation and followed by mild mechanical treatment to produce ultrafine cellulose nanofibers for fabrication of nanofibrous membranes. However, the hydroxyl groups in cellulose molecules are partially oxidized to introduce new carboxylate and aldehyde functional groups.[11] The chemical extraction of nanocellulose using acid hydrolysis is usually appropriate for obtaining nanostructures from original raw materials and involves the use of highly concentrated chemicals in addition to a series of repetitious steps.[12] Hence, it is imperative that direct approaches which do not involve the complete dissolution of cellulose molecules, plus preserve the originality of the cellulose structure as well as its chemical properties of the surface hydroxyl groups are further explored.

High intensity ultrasonication (HIUS) is a well-developed physical process and represents by far the most favorable and efficient mechanical method for the manufacture of cellulose nanofibrils as well as other nanostructured materials.[13,14] The sonochemical synthesis of various nanostructured inorganic materials have also been reported for instance.[15] This method has been employed for the fibrillation of cellulose with nanoscale structures, the majority of which have primarily been produced from natural raw material sources.[16–21] Different dimensions of cellulose nanostructures are realized depending on the starting material, operating conditions and pretreatments used. HIUS has the advantage of maintaining the originality of the fibers in terms of length and structure.[16] However, reports using the commercially available α-cellulose for cellulose nanofibrillation by HIUS and explicit elucidation of its resultant morphologies is sufficiently lacking. Correspondingly, direct filtration technology for fabricating thin nanoporous membranes using one-dimensional (1D) and two-dimensional (2D) polymer nanofibers dispersions produced in this way is hardly reported. It has been suggested that appropriate pretreatments of cellulose before mechanical fibrillation is necessary to promote the accessibility of hydroxyl groups, increase the inner surface, alter crystallinity, and break up cellulose hydrogen bonds and thus boost the reactivity of the fibers.[22] Meanwhile, due to the highly hydrophilic nature of the cellulose fibers, surface modification is an inherent challenge to the compatibly and adhesion of cellulose nanofibers to both polymeric and nonpolymeric materials.[23] As chemical treatment can improve the interface bonding along with eliminating any existent impurities in the fibers, a treatment regime that does not lead to the destruction of the cellulose structure must be taken into consideration.

Herein, we report a facial approach combining pre-chemical and HIUS mechanical treatment to prepare cellulose nanofibers from commercially available α-cellulose. Primal focus was directed toward understanding the effect of pre-alkaline treatment with sodium hydroxide on the formation and morphology of the as-prepared nanofibers. Furthermore, these nanofibers were used to fabricate nanofibrous nanoporous membranes on a macroporous support by the direct filtration method. The membranes structure and separation performances were explicitly characterized. The as-fabricated membranes with a controllable membrane thickness show ultrahigh permeation fluxes and good UF performances. The current work demonstrates a direct approach to the fabrication of efficient UF support membranes that have great potential applications for filtration and size-selective separations.

## EXPERIMENTAL

### Materials

Commercial α-cellulose powder purchased from *Sigma-Aldrich* was used as the raw material to produce cellulose nanofibers. Microfiltration filters of cellulose acetate (CA), with a cut-off of 0.2 $\mu$m and 25 mm in diameter, were purchased from *Sartotius Stedim Biotech*. Gold nanoparticle solution and ferritin (from equine spleen) were obtained from *British Biocell International* and *Sigma-Aldrich*, respectively. Ultrapure water was utilized for the preparation of aqueous solutions of sodium hydroxide (NaOH) and hydrochloric acid (HCl). These analytical grade chemicals were purchased from *Sinopharm Chemical Reagent Co. Ltd.* (Shanghai, China).

### Preparation of Cellulose Nanofibers

Typically, 0.2200 g of α-cellulose was dispersed in 200 mL of ultrapure water contained in a 250 mL beaker under constant magnetic stirring overnight. The sample was filtered using a filter paper and the solid was extracted in 150 mL of sodium hydroxide with stirring at 60 °C for 40 min to break up the intermolecular bonds in the cellulose. Different concentrations of sodium hydroxide used were designated as *x* wt %, where *x* is 0, 2, 5, 7.5, 10, and 17.5. This was carried out with the attempt to understand the effect of alkaline concentration on the formation and structure of the resultant nanofibers. Each of the alkaline treated samples was filtered and washed with ultrapure water until neutral. All the samples then underwent subsequent dispersion in 150 mL of a 10 wt % hydrochloric acid solution under magnetic stirring at 60 °C for 2 h to break up the amorphous regions of cellulose and neutralize any residual sodium hydroxide in the α-cellulose. The resulting solid after filtration was thoroughly washed with ultrapure water until neutral to obtain pre-treated α-cellulose.

The pre-treated cellulose was dispersed in 350 mL of ultrapure water and then subjected to ultrasonic treatment for 45 min using a vibra-cell ultrasonic processor (Model VCX500, *Sonics & Materials, Inc.*, The United States). The resulting transparent colloidal suspension was further centrifuged at 120,000 rpm for 10 min to obtain cellulose nanofibers dispersion. The content of cellulose nanofiber (*C*, wt %) in its dispersion was estimated by the method from a previous work.[24] The following equation was applied:

$$C(\text{wt}\,\%) = \frac{w_0 - w_1}{W_m + (w_0 - w_1)} \quad (1)$$

where $W_m$ is the weight of the dispersant, $w_0$ is the weight of the original cellulose powder, and $w_1$ is the weight of the large separated-out cellulose fibers that were collected after centrifugation and dried to constant weight at 60 °C for 1 day. Finally, a transparent suspension of cellulose nanofibers containing about 0.024 wt % α-cellulose content was obtained and stored at 5 °C. The cellulose nanofibers dispersion was stable for over a week. Only a single ultrasonic bath agitation was necessary to produce a uniform dispersion for membrane fabrication.

### Characterization of Cellulose Nanofibers

Scanning electron microscopy (SEM) (*Zeiss*, Sigma) was employed to elucidate the structural morphology of the cellulose nanofibers. Transmission electron microscopy (TEM) (JEM-2100F, 200 kV, *JEOL*, Japan) was used to ascertain the dimensions and confirm the formation of cellulose nanofibers. The samples for SEM were first prepared by filtering 5 mL of the nanofiber dispersion on a CA filter, dried in air, and then gold coated using a JFC-1600 auto fine coater to prevent charging and improve the membranes' electroconductivity. For TEM analysis, cellulose nanofibers dispersion was initially dropped on a copper grid coated with a carbon film and dried in the air to obtain the sample for observation.

X-ray diffraction (XRD) was performed to examine the crystallinity of the cellulose nanofibers. The spectra of the original cellulose and the chemically pre-treated cellulose were recorded on a XRD system (Ultima IV, *Rigaku Corporation*, Japan) using Nickel filtered Cu-$K\alpha$ radiation at operating voltage of 40 kV, a current of 30 mA and a scan speed of 10° $\text{min}^{-1}$. The crystallinity index was calculated following the empirical height method proposed by Segal.[25]

$$C_{rI} = \frac{I_{200} - I_{am}}{I_{200}} \times 100\% \quad (2)$$

where $C_{rI}$ is the relative degree of crystallinity, $I_{200}$ is the maximum intensity of 200 lattice diffraction at $2\theta = 22.5°$, and $I_{am}$ is the intensity of diffraction in the same units at $2\theta = 16.5°$.

Fourier transform infrared spectroscopy (FT-IR) was used to study the chemical structure of the cellulose after the chemical treatments. The samples prior to analysis were initially mixed with potassium bromide (KBr) at a ratio of 1 wt % of sample to 99 wt % of KBr. The samples were then pressed into discs to achieve a planar surface and subsequently subjected to FT-IR measurement using an FT-IR Nicollet 380 spectrometer. Furthermore, the thermal stability of the samples subjected to the different pretreatments was determined using a Standard SDT (simultaneous thermogravimetric analyzer and differential scanning calorimeter) instrument (SDT Q600 series) with a heating rate of 10.00 °C/min under a nitrogen atmosphere.

### Fabrication of Cellulose Nanofibrous Membranes

The cellulose nanofibrous membranes were fabricated using the approach described previously.[24,26] A given volume of the as-prepared cellulose nanofiber dispersion was suction filtered over a CA filter with a cut-off of 0.2 μm. During filtration, the cellulose nanofibers were expected to evenly distribute over the surface of the substrate support and form an ultrathin nanoporous film. Both the surface topography and the cross-section morphology of the resulting membranes were examined using SEM. The samples for cross-section observation were first freeze-fractured in liquid nitrogen and all the samples were gold coated as above. The membrane thickness was estimated during SEM characterization and the MeasureIT software (*Olympus Soft Imaging Solutions Gmbh*, Germany).

### Separation Experiments Using Cellulose Nanofibrous Membranes

UF experiments were performed using a glass filter holder in a dead-end mode (Supporting Information Figure S1). The pure water flux (PWF) ($J$, $\text{L/m}^2\text{/h/bar}$) was evaluated by filtering 100 mL of ultrapure water across the membrane, and calculated by

$$J = V/(AtP) \quad (3)$$

where $V$ is the water volume (L), $A$ is the effective membrane filtration area ($\text{m}^2$), $t$ is the filtration time (h), and $p$ is the suction pressure across the membrane (bar). To evaluate the separation properties of the as-fabricated membranes, 15 mL of 20.0 mg/mL ferritin (12 nm, protein molecule) and 10 nm gold nanoparticle solutions were filtered across the membrane using a glass filter holder at a suction vacuum pressure of 80 kPa.[26] A model synthetic textile effluent was used to further quantify the separation performance.

We performed decolorizing experiments by filtering a predetermined volume of a 10.0 mg/L (μg/mL) methylene blue solution across the fabricated membranes using a transmembrane pressure of 0.8 bar. The feed, permeate and concentrate were characterized using an ultraviolet and visible (UV–vis) spectrophotometer (Model UV-1800 series, *Shimadzu*, Japan). The rejection efficiency ($R$, %) was calculated by

$$R = (1 - C_i/C_0) \times 100\% \quad (4)$$

where $C_i$ and $C_0$ are the concentrations in the permeate and the feed, respectively. The dye adsorbed (decolorized) and the adsorption capacity were calculated in a similar way following the previous method.[27,28]

## RESULTS AND DISCUSSION

### Preparation of Cellulose Nanofibers

Pre-chemical treatments of α-cellulose was performed to improve the fiber matrix interface adhesion, achieve a better fiber wetting, aid, and ease the fibrillation of cellulose fibers by ultrasonication and increase the crystallinity of the resultant nanofibers. Figure 1(a) shows the schematic for the preparation of the cellulose nanofibers. Pre-treatment results in swelled, loose, and purified fibers making them more vulnerable to fibrillation by subsequent ultrasonication.[14] The intermolecular bonding between the several cellulose chains aligned by covalently linked side by side bond conformation gives rise to a strong entangledlike network structure of its fibers. The sodium hydroxide hydrates have the power to penetrate and bring about the stretching of these intermolecular hydrogen bonding networks, resulting in either partially damaged or weakened bonds to produce freely loose or straightened fibers. The hydrochloric

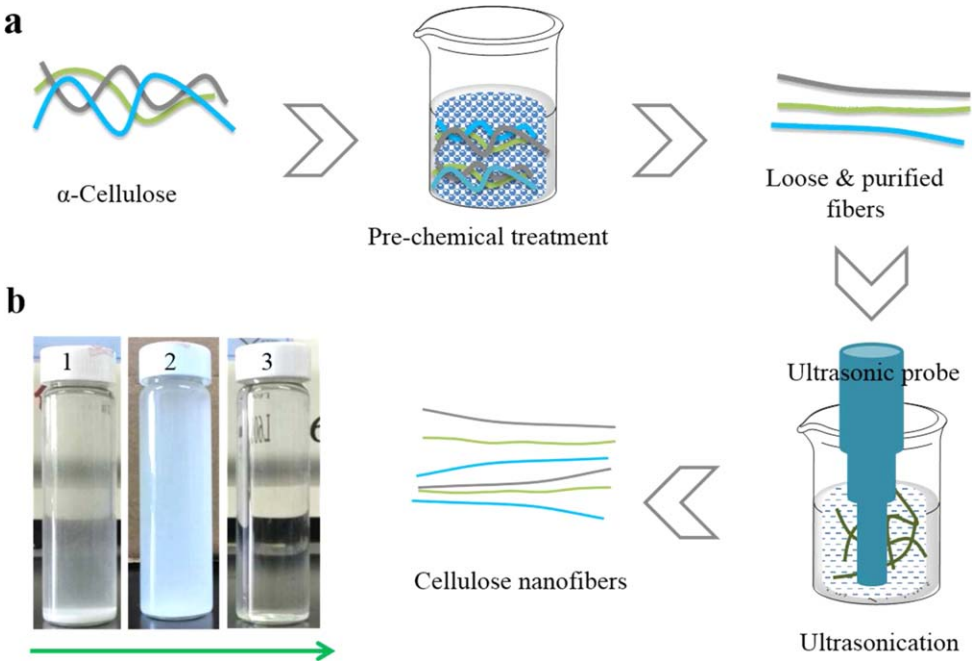


**Figure 1.** Preparation of cellulose nanofibers. (a) Schematic procedure for the nanofiber preparation by ultrasonication. (b) Digital photos of nanofiber preparation: (1) before ultrasonication, (2) after sonication, and (3) after sonication plus centrifugation. [Color figure can be viewed in the online issue, which is available at wileyonlinelibrary.com.]

acid then easily dissolves the amorphous regions, extractives, and any prevailing impurities into solution, which are expelled in filtration to produce purified fibers. During ultrasonic treatment, the yield of the nanofibers was expected to increase and in order to ascertain this; an untreated sample was directly ultrasonicated without pre-chemical treatment for comparison. The untreated sample gave a yield of about 0.01365 wt % cellulose content representing 16.70% of the original weight. In contrast, a cellulose content of about 0.02422 wt % corresponding to 27.03% of the original weight was yielded by the treated sample.

The suspension in bottle 1 containing cellulose fibers before sonication displays a distinguishable aqueous and settled-out solids phases. After sonication, a cloudy but translucent colloidal suspension in bottle 2 is obtained. And the resultant suspension after centrifugation in bottle 3 is the expected clear and transparent cellulose nanofibers dispersion [Figure 1(b)]. This implied that the nanofibers had been successfully obtained following the sonication treatment. The crystalline cellulose fibers in suspension are distorted and disintegrated by high mechanical oscillating hydrodynamic forces produced by high-frequency acoustical energy generated by the ultrasonic processor. It is known that the mechanism of sonication occurs by cavitation, which comprises the formation, growth, and collapse of cavities (bubbles) when the molecules in a liquid (suspension) absorb ultrasonic energy.[15]

Concurrently, the potential energy of the expanded bubbles is transformed into the kinetic energy of a liquid jet in violent shock waves applied on the surfaces of fibers. This causes the breakage of weak intermolecular bonding among the solid cellulose fiber aggregates in the suspension.[14] subsequently, the weakened bonding forces following the prechemical treatment should result in more fibrillation of the treated than the untreated fibers. The generated ultrasonic waves uniformly disperse the nanofibers in suspension. No appreciable amount of yield was realized with increased time of sonication suggesting that the chosen time was appropriate for the fibrillation of α-cellulose.

### Structure and Properties of Cellulose Nanofibers

**TEM Characterization.** This was performed to confirm the production of the cellulose nanofibers. Figure 2(a) shows a TEM image of the obtained cellulose nanofibers via pre-treatment with 5 wt % sodium hydroxide solution. Individually dispersed and singularly aligned or partially agglomerated into buddlelike nanofibers can be clearly observed. These nanofibers exhibit dimensions ranging from 10 to 40 nm with an average diameter of about 20 nm, as shown in Figure 2(b). The agglomeration tendency is an expected occurrence given the nature of the high specific surface area of the produced nanofibers. This also occurs in combination with the strong interactions resulting from the intra- and intermolecular hydrogen bonds that are an existent property of native cellulose fibers. Such cellulose nanofiber agglomeration was also observed in the nanofibers suspension after a prolonged period of standing. Due to the nature of their dimensions, it was expected that the nanofibers should freely form thin nanoporous films on a microporous support during filtration.

**SEM Observation.** As shown in Figure 3, SEM observation is consistent with that of TEM. But the morphology of the nanofibers is revealed to be highly influenced and dependent on the concentration of the NaOH employed during the pre-alkaline treatment. The micrographs resulting from both with mild

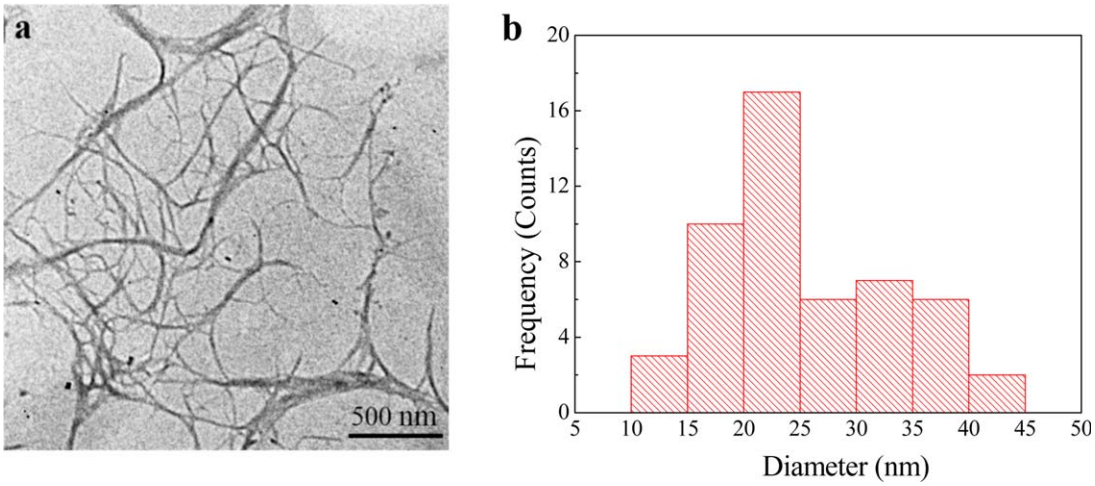


**Figure 2.** TEM micrograph of cellulose nanofibers (**a**) and diameter distribution histogram of the cellulose nanofibers (**b**). The diameters were directly estimated using the MeasureIT software. [Color figure can be viewed in the online issue, which is available at wileyonlinelibrary.com.]

prealkaline and no alkaline treatments reveal the formation of a network of long and interconnected fine cellulose nanofibers. They are also orderly distributed and fully covered on the surface of support membrane [Figure 3(a,b)]. Above 5 wt % concentration, the micrographs show the formation of a very dense and highly agglomerated netlike bundle of nanofibers. There are hardly any visible characteristic porelike conformations on the surface of the membrane formed from the 7.5 wt % treated fibers [Figure 3(c)]. For the membrane formed from the 17.5 wt % treated fibers, some nanocrystallike structures can be observed on the surface and although with a decreased size, the mercerized fibers lead to formation of a rough surface topology [Figure 3(d)]. Overall, these observations confirm the successful production of cellulose nanofibers from α-cellulose via ultrasonication.

**XRD Analysis.** Figure 4(a) shows the XRD diffractograms of the original α-cellulose and the chemically pretreated fibers at different alkaline concentrations. The pre-chemical treatment of the cellulose fibers has a significant influence on the crystal type of cellulose as well as its crystallinity and the crystallinity index. Clearly, except for the differences in their intensities, there is no

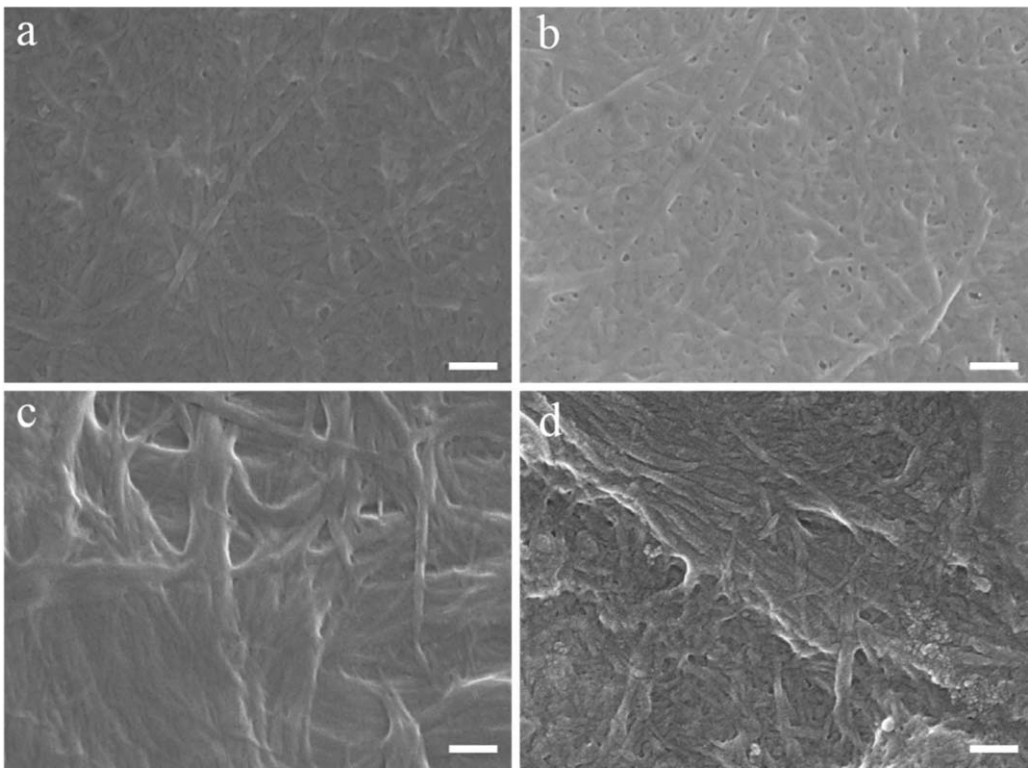


**Figure 3.** SEM images of the cellulose nanofibers of untreated (0 wt %) (**a**) and via pre-treatment with 5 wt % (**b**), 7.5 wt % (**c**), and 17.5 wt % (**d**) sodium hydroxide. The scale bar is 200 nm.

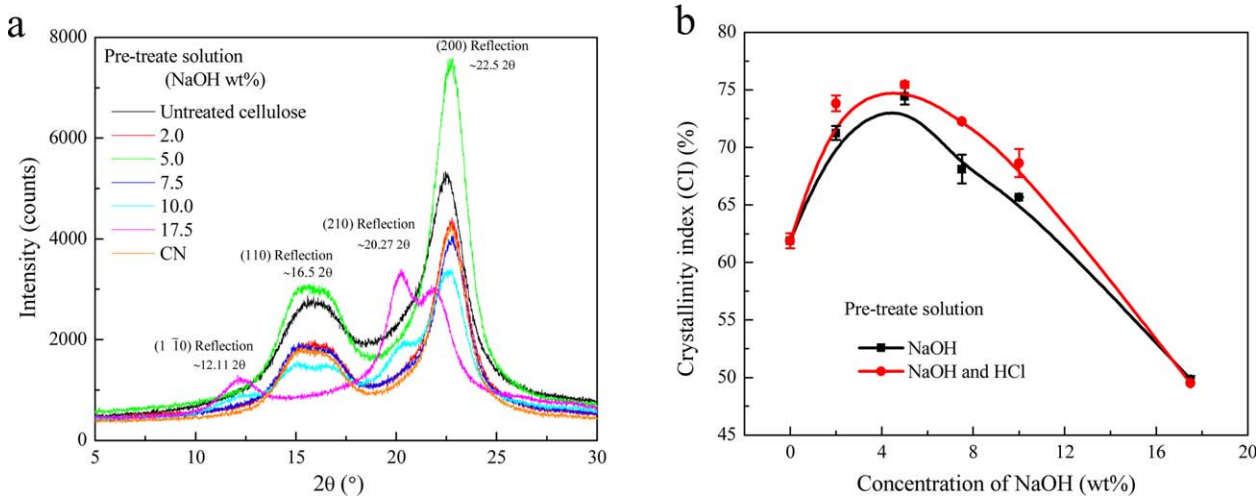


**Figure 4.** X-ray diffraction patterns (**a**) and variation of the crystallinity index (**b**) of treated α-cellulose under different concentrations of sodium hydroxide. CN indicates the diffraction pattern of cellulose nanofibers obtained after ultrasonication for the optimized 5 wt % NaOH treated α-cellulose. A total of three sample scans were obtained and the average of the results was recorded. [Color figure can be viewed in the online issue, which is available at wileyonlinelibrary.com.]

remarkable change in the diffractograms between the fibers treated with 0, 2, and 5 wt % sodium hydroxide. The diffractograms exhibit a typical cellulose type I structure characterized by the appearance of wide diffraction peaks at around 22.5° and 16.5° corresponding to the crystallographic planes 200 and 110, respectively. However at high concentration, there is a shift in the main peak of original cellulose to a cellulose type II structure [with typical diffraction peaks at around 12.11° (110) and 20.27° (210)] for the fibers treated with 17.5 wt % sodium hydroxide.[29,30] As shown in Figure 4(b), the computation of the crystallinity indicates that the crystallinity index initially increases with increasing alkaline concentration. The crystallinity index increased from an initial value of 62% of the original α-cellulose to a maximum of about 75% following a prealkaline treatment with 5 wt % sodium hydroxide. A further increase in the alkaline concentration beyond 5 wt % results in the crystallinity index being gradually decreased down to about 50% at high alkaline concentration (17.5 wt %), suggesting a change in cellulose structure from crystalline to amorphous. These results are consistent with previous work undertaken on the mercerization of cellulose.[31]

At a low alkaline concentration, the power of sodium hydrates is weak to distort the cellulose fibrils. However, there is a rearrangement resulting from the swelling and decrystallization of intra- and intermolecular bonds of the cellulose lattice structure. By increasing the alkaline concentration, the intermolecular bonds are progressively weakened by the further swelling and penetration of sodium hydrates inside the cellulose fiber matrix. This leads to the realignment and complete recrystallization of cellulose fibers to break the existent intermolecular chain links to produce new crystalline lattice structures in the cellulose chain links.[32] The treatment under mild acid hydrolysis was observed to further slightly boost the crystallinity index of cellulose fibers [Figure 4(b)]. This increase was however not much pronounced like that observed when only alkaline treatment was performed. This could be attributed to the break up and removal of a proportion of amorphous regions and some extractives still present in the α-cellulose. The changeless main peak of cellulose diffractograms also further affirms the fact that this treatment has little influence on the alteration of the cellulose crystal structure but only dissolves the amorphous regions. Likewise, ultrasonication does not affect the crystal integrity of the optimized pretreated sample since there was no observable alteration in the XRD patterns of the cellulose nanofibers (CN) obtained after ultrasonication and that of the original untreated α-cellulose fibers. Generally, the increase in the crystallinity of the cellulose nanofibers over that of the original cellulose fibers is an essential requirement in their applications in membrane separation and composite reinforcement of materials.[6] Consequently, the mild prechemical treatment of cellulose fibers is imperative to prepare the cellulose nanofibers.

**FT-IR Analysis.** FT-IR spectroscopy can be used to construe the variations in the structure and chemical composition of elements subjected to different chemical treatments. Figure 5(a) shows the FT-IR spectra of the cellulose treated under the different sodium hydroxide concentrations. The characteristic bands related to the physical and chemical changes occurring in the cellulose as listed in Supporting Information Table S1 are the O—H stretching at between 4000 and 2995 $cm^{-1}$, the O—H bending of adsorbed water at 1645 $cm^{-1}$, the C—H stretching at 2904 $cm^{-1}$, the H—C—H and O—C—H in-plane bending vibrations at 1431 $cm^{-1}$, the C—H deformation vibration at 1373 $cm^{-1}$, the C—O—C, C—C—O, and C—C—H deformation modes and stretching vibrations in which the motions of the C5 and C6 atoms are at 914 $cm^{-1}$.[33] Compared with the original α-cellulose powder, there is a presence of increasing amount of amorphous cellulosic samples indicated by the characteristic peaks of hydrogen bonds becoming sharper with strong decrease in the band intensity as the alkaline concentration increases. This is also confirmed by the slight shift of the band from 2900 $cm^{-1}$ (Supporting Information Table S1), corresponding to the C—H stretching vibration, to higher wavenumber values

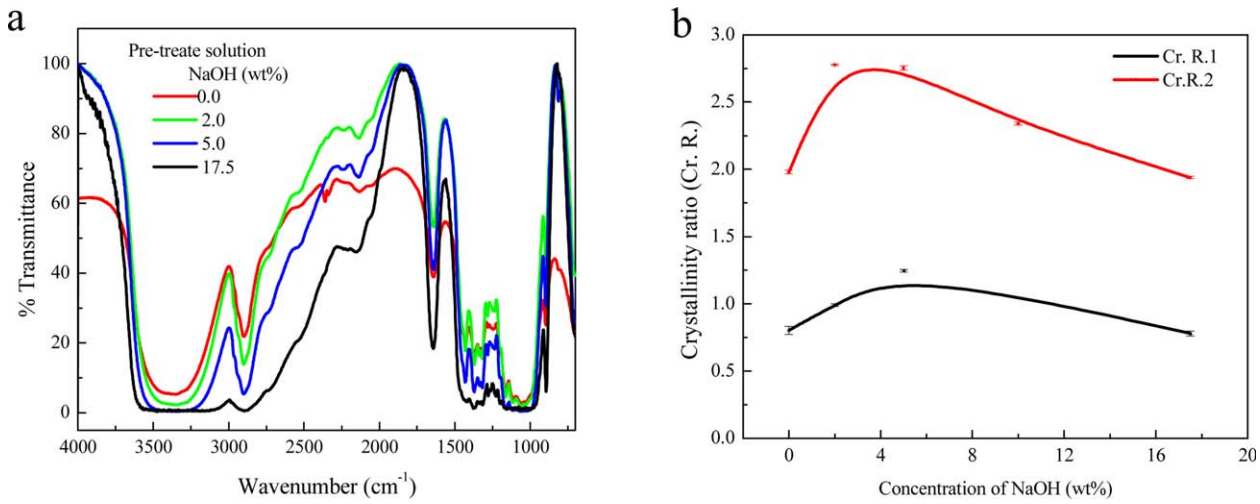


**Figure 5.** The transmittance FT-IR spectra (**a**), and variation of the crystallinity ratio (**b**) of α-cellulose treated with different alkaline concentrations. A total of three sample scans were obtained and the average of the results was recorded. [Color figure can be viewed in the online issue, which is available at wileyonlinelibrary.com.]

and must be attributed to the gradual breakup of the intra- and intermolecular hydrogen bonds. The effect of prechemical treatment on the production of cellulose nanofibers during the sonication process could partly be explained by the above observation.

Of specific importance are the bands occurring at about 4000–2995 $cm^{-1}$, 2904 $cm^{-1}$, 1431 $cm^{-1}$, 1373 $cm^{-1}$, and 897 $cm^{-1}$, which are particularly sensitive to the state of the crystalline and amorphous regions.[29,31] For the 17.5 wt % NaOH treated fibers, the symmetric $CH_2$ bending vibration band (1431 $cm^{-1}$) decreases, and the C—O—C stretching at $\beta$-(1-4)-glycosidic linkages (around 897 $cm^{-1}$) increases (Supporting Information Figure S2). This decrease in the crystallinity band (1431 $cm^{-1}$) and increase in the amorphous band (897 $cm^{-1}$) indicates the reduction in the degree of crystallinity and the increasing intensity of the amorphous content in the samples, respectively. Moreover the increase in the absorbance at about 897 $cm^{-1}$ is a confirmation of the transformation of the cellulose type (I) to cellulose type (II) lattice structure at high alkaline concentration.[28] The absorbance peak at 1431 $cm^{-1}$ is the highest and the lowest for the 5 wt % and 17.5 wt % NaOH treated fibers respectively. The calculated crystallinity ratios using two methods: the absorbance ratio from 1372 $cm^{-1}$ (A1372) to 2900 $cm^{-1}$ (A2900) bands: Cr.R.1 = A1372/A2900 and the absorbance ratio from 1430 $cm^{-1}$ (A1430) to 893 $cm^{-1}$ (A893) bands: Cr.R.2 = A1430/A893 is shown in Figure 5(b). Clearly, the ratio of crystallinity for 5 wt % treated cellulose of 1.246 and 2.752 are higher than that of 0.779 and 1.94 for the 17.5 wt % treated fibers for both of the methods used, respectively. This result is practically in good agreement with that obtained by XRD analysis. And taken together with the morphological results, it suggests that 5 wt % would be the most appropriate concentration for the prealkaline treatment of α-cellulose prior to ultrasonic nanofibrillation.

**Thermal Stability Analysis.** Figure 6 shows the thermogravimetric analysis (TGA) and differential scanning calorimeter (DSC) curves of untreated α-cellulose, the optimized 5 wt % NaOH pretreated α-cellulose and cellulose nanofibers obtained after ultrasonication. The temperatures at 10 wt % weight loss ($T_{10}$) and 50 wt % weight loss ($T_{50}$) of the untreated α-cellulose fibers were 300.54 °C and 342.90 °C. On the other hand, the $T_{10}$ and $T_{50}$ of the chemically treated fibers were, respectively, 284.19 °C and 315.95 °C. The cellulose nanofibers obtained after ultrasonication have $T_{10}$ and $T_{50}$ of 305.36 °C and 328.19 °C, respectively.

The thermal stability of untreated α-cellulose is depressed after the chemical pretreatments. This is attributed to the effect of sodium hydroxide on α-cellulose as explained previously. This was important in the fibrillation of the fibers during the ultrasonication step and is consistent with the increased yield of the nanofibers after the sonication. As the melting point temperature, $T_m$ depends on the molecular weight of the polymer, the lower melting points of the samples after chemical treatments; suggest that the molecular weight of the original α-cellulose slightly decreased after the pretreatments. Meanwhile, the samples present an endotherm of fusion which confirms the crystalline character of the samples as revealed by XRD. The peak of endotherm represents the melt peak temperature of the samples. As the endothermic dip in the DSC curve is greater for the cellulose nanofibers, it suggests that the overall crystallinity of the nanofibers after the treatments is much improved in comparison to that of untreated α-cellulose. Overall, these results suggest that the resultant cellulose nanofibers exhibit good thermal stability of above 200 °C and improved crystallinity which corroborates well with the XRD and FT-IR data.

**Fabrication of Cellulose Nanofibrous Membranes**

In consideration of the yield, the highest obtainable crystallinity index and without significant changes to the overall crystallinity of the resultant nanofibers via sonication, 5 wt % was chosen as the optimal sodium hydroxide concentration to pretreat the cellulose fibers. The cellulose nanofibers were first uniformly dispersed in an ultrasonic bath for 20 min and then

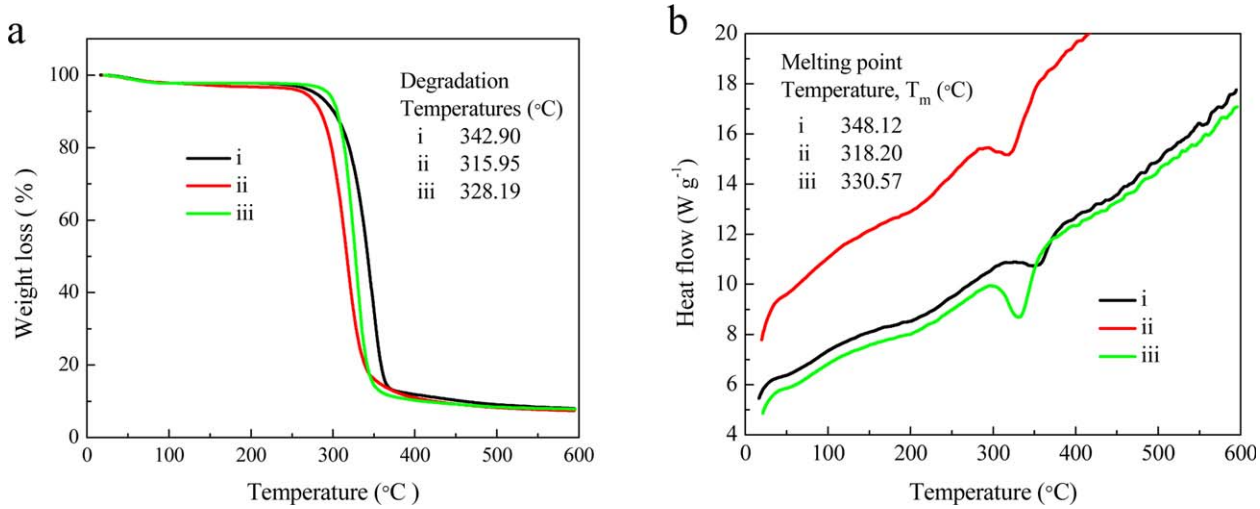


**Figure 6.** TGA curves and degradation temperatures (**a**), DSC curves and melting temperatures of (i) untreated α-cellulose, (ii) 5 wt % NaOH pretreated α-cellulose, and (iii) cellulose nanofibers after ultrasonication. [Color figure can be viewed in the online issue, which is available at wileyonlinelibrary.com.]

predetermined amounts were filtered across the support to form the nanofibrous membranes. The representative SEM images are shown in Figure 7. The left side images a, b, c, and d, represent the surface SEM micrographs of membranes fabricated from 5, 10, 15, and 20 mL of cellulose nanofibers dispersion, respectively. The corresponding right side images represent their respective cross sections. The surface topographic SEM micrographs reveal the orderly distribution of a network of fine, long, and interconnected netlike cellulose nanofibers that fully cover the surface of support. The interconnectivity of the nanofibers gives rise to the porelike conformation that is characteristic of a nanoporous structure. There is no significant difference in the morphology of membranes fabricated from the different volumes of nanofibers dispersion except for the agglomerations which, is attributed to the accretion of the nanofibers. The cross-sectional images reveal that the cellulose nanofibers freely assemble on the surface of the support forming a barrier layer with a typical asymmetric membrane structure.

The nanofibrous layer thickness increases with increasing volume of the nanofibers dispersion filtered. The lowest thickness of about 496 nm was obtained for membrane prepared from 5 mL of nanofibers dispersion and the highest thickness of about 564 nm was obtained from 20 mL of nanofibers dispersion. The weight and thickness between the consecutive membranes was not consistent due to the loss of some very tiny nanofibers into the filtrate solution. During filtration of the cellulose nanofibers dispersion, the accretion of the nanofibers reduce the space between them and subsequently the corresponding effective pore size of the resultant membranes was expected to decrease with increase in the amount of the nanofibers dispersion filtered.

Hence, it was expected that flux should decrease with increasing membrane thickness during pressure driven separation. The membranes are also hydrophilic following the incorporation of cellulose nanofibers. This is evidenced by ease of their wettability as characterized by the water contact angle measurements. As shown in Figure 8(a), there is a the drastic decrease in the water contact angle from 90.9° for the support membrane to 53.6°, 47.0°, 43.5°, and 38.2° for membranes fabricated from 20, 15, 10, and 5 mL of cellulose nanofibers, respectively. This

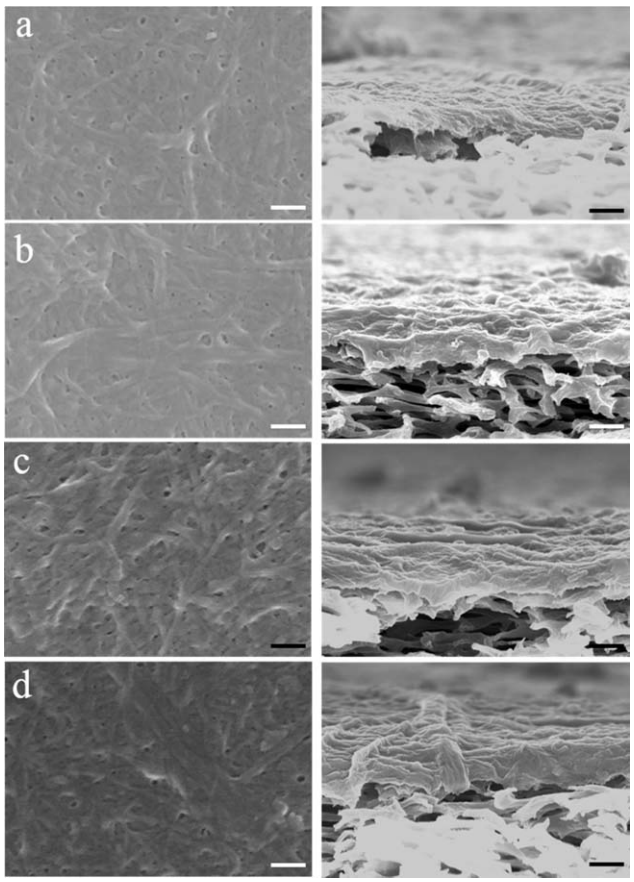


**Figure 7.** Representative top surface morphologies (left) and cross-sectional (right) SEM micrographs of the membranes prepared from 5 mL (a), 10 mL (b), 15 mL (c), and 20 mL (d); of cellulose nanofibers dispersion. The scale bar is 200 nm.

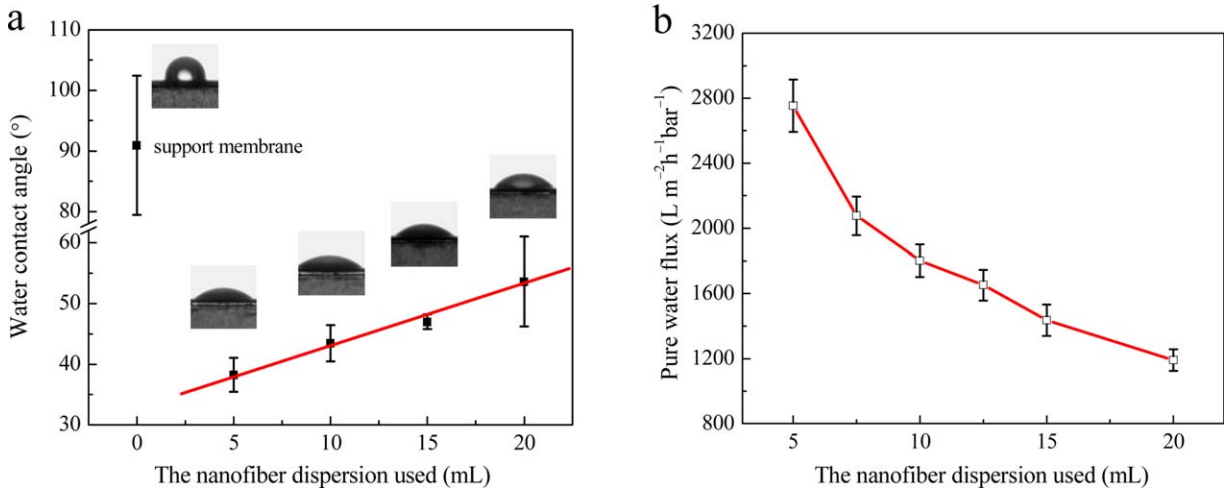


**Figure 8.** Water contact angles (**a**) and the pure water flux (**b**) of membranes prepared with different volume of nanofibers dispersion. The insert photos are the representative water contact angle images. [Color figure can be viewed in the online issue, which is available at wileyonlinelibrary.com.]

surface wetting property is paramount in the membranes separation capabilities.

### Separation Performances of Cellulose Nanofibrous Membranes

The membrane filtration performance is an essential requirement of porous membranes, as this translates to high efficient purification and energy savings in industry. Table I lists the separation performances of the cellulose nanofibrous membranes. The membranes exhibit high water flux that is attributed to the high wettability of the cellulose nanofibers surface owing to the hydrophilic cellulose. The plot of the water flux of the fabricated membranes is shown in Figure 8(b). Generally, the observed flux is inversely proportional to the membrane thickness (volume of nanofibers dispersion filtered), which is in accordance with the Hagen–Poiseuille equation of incompressible flow through circular pipes. There is a sharp drop in the flux from 2.75 to 2.08 $\times$ $10^3$ L/m$^2$/h/bar between membranes prepared from 5 and 7.5 mL of the nanofibers dispersion, respectively. Then the flux continues to linearly decrease with increase in the amount of cellulose nanofibers dispersion filtered, to 1.44 $\times$ $10^3$ L/m$^2$/h/bar for the membrane prepared from 15 mL.

The above trend is consistent with the water contact angle measurements. A few nanofibers (5 mL) on the surface of the support membrane form a thin layer that is easily wetted resulting to the corresponding high water flux. But a high volume of nanofibers filtered (10–20 mL) forms a less thin barrier layer, which is less easily wetted and hence the observed decreases in the water flux. A decrease in flux with increasing membrane thickness is an expected occurrence as described previously. This is because the mass transfer resistance that is entirely contributed by the cellulose nanofiber barrier layer increases with increasing quantity of nanofibers filtered.[26] This observed trend is consistent with many other reports in literature.[10,11] The water flux of 2.08 $\times$ $10^3$ L/m$^2$/h/bar above is on the order of more eight times higher than that of some typical porous UF membranes. For instance a water flux of 190 L/m$^2$/h was obtained for a polystyrene nanoparticle membrane at a pressure difference of 80 kPa whereas a PWF of 200 L/m$^2$/bar/h is reported for a porous and interconnected PBI/P84 UF membrane.[34,35]

The purification of proteins and separation of nanosized particles is one of the functions of nanoporous membranes. We carried out nanoparticle separation to ascertain the separation characteristics of the as-prepared cellulose nanofibrous membranes. Solutions containing ferritin molecules (12 nm) and 10-nm gold nanoparticles were permeated through the as-prepared membranes. Unlike in the case of water flux, the rejections for these neutral molecules are not largely dependent on the

**Table I.** Separation Performances of the Cellulose Nanofibrous Membranes

| Nanofibers (mL) | Thickness (nm) | Porosity (%) | $J_{water}$ ($10^3$ L/m$^2$/h/bar) | Rejection (%) | |
|---|---|---|---|---|---|
| | | | | 10 nm gold | Ferritin |
| 5.0 | ~496 | ~68.5 | 2.75 ± 0.16 | 84.6 ± 0.3 | 94.3 ± 0.6 |
| 7.5 | ~512 | ~67.7 | 2.08 ± 0.12 | 93.0 ± 0.2 | 92.8 ± 1.3 |
| 10.0 | ~528 | ~66.9 | 1.80 ± 0.10 | 91.5 ± 0.2 | 91.3 ± 3.2 |
| 12.5 | ~547 | ~66.4 | 1.65 ± 0.10 | 93.0 ± 0.4 | 90.8 ± 0.2 |
| 15.0 | ~556 | ~65.1 | 1.44 ± 0.10 | 93.5 ± 5.2 | 92.5 ± 1.8 |
| 20.0 | ~564 | ~55.8 | 1.19 ± 0.07 | 93.2 ± 1.8 | 90.2 ± 4.8 |

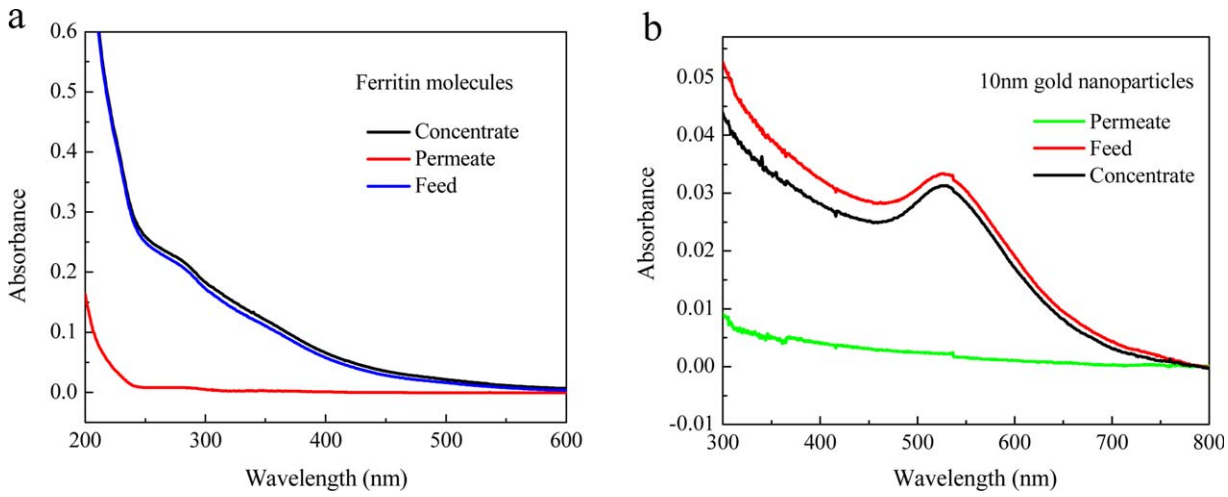


**Figure 9.** UV–vis absorption spectra of the concentrate, feed, and permeate of ferritin (**a**) and 10-nm gold nanoparticle (**b**) solutions through the membranes prepared from 10 mL of dispersion. [Color figure can be viewed in the online issue, which is available at wileyonlinelibrary.com.]

increase in the quantity of the nanofibers dispersion filtered (Table I). Specifically, the rejection of ferritin seems to decrease with increase in the membrane thickness, that is, the highest ferritin rejection of 94.3% was obtained by the membrane prepared from 5 mL of nanofibers dispersion, whereas the lowest rejection of 90.2% was obtained by the membrane prepared from 20 mL of dispersion. This unexpected trend could be attributed to the increased reactivity of the surface OH groups following pre-alkaline treatment that enhanced the hydrogen bonding interactions between the cellulose nanofibers. So, the nanofibers had a high propensity to agglomerate as more fibers assembled on the surface of the support. These cellulose nanofibers agglomerations were also revealed by the SEM images. As a consequence, the filtration of more nanofibers could have resulted in the creation of some cavities that allowed more ferritin to pass through than could be adsorbed on the surface of the nanofibers and hence low rejection.

Meanwhile, when a small volume is filtered, the few nanofibers are evenly distributed over the surface of the microporous support. There is less agglomeration and more ferritin molecules are adsorbed on the surface of nanofibers leading to a high rejection. In the same vein, the membranes also have good rejection for 10-nm gold nanoparticles and ferritin molecules as shown in Figure 9. Comparing the differences between the UV absorbance spectra before and after separation clearly shows that there is increasing difficulty in the separation of the solutions, that is, both the ferritin molecules and 10-nm gold nanoparticles have difficulty in passing through the membranes. Therefore, on account of the rejections in Table I being all above 90% except for the membrane prepared from 5 mL nanofibers dispersion and as monodispersions of inert nanoparticles have been conveniently used to determine the pore size distribution in a variety of UF membranes, it suggests that the effective pore size (cut-off) of the as-prepared membranes is below 10 nm.[36,37]

### Decolorization of Methylene Blue (MB)

Methylene blue (MB) which is a member of the cationic dyestuffs has several applications in the chemical industry including; redox reaction indicator in laboratory titrations, dye in the textile industry, or stain in biological assays. The use of this chemical in one way or another, results in the generation of waste which presents an inevitable task for treatment to avoid its adverse impacts to the environment and consequently to human health. Whereas dye removal by physical adsorption methods has been well studied, the expensive nature of the wastewater treatment process in industry necessitates the application of easily obtainable and biodegradable materials to reduce costs and curb further pollution.

In order to demonstrate their applicability for typical industrial wastewater treatment, the fabricated cellulose nanofibrous membranes were used to decolorize MB by filtration via dead end mode. The MB separation performance of the as-prepared membranes is summarized in Figure 10. The decolorization of the MB decreased with increase in the volume of the feed solution filtered across the membranes. As shown in Figure 10(a), the decrease in the peak intensity of the UV spectra in moving from the original 10 mg/L MB solution down to 1 mL [i.e., MB (10 mg/L] > 15 mL > 10 mL > 6 mL > 3 mL > 1 mL] is ascribed to MB adsorption on the surface of the as-prepared membranes. Visual observation in which the characteristic bluish color of the original MB solution is readily decolorized to a clear filtrate obtained after a single filtration through the membrane is shown in Supporting Information Figure S3, ASI.

Notably, the MB decolorization efficiency of the membranes is remarkably enhanced at high pH of the nanofibers dispersion. Computation of the dye removal efficiency in Figure 10(b) reveals that at the pH of 6 of the original nanofibers dispersion, the membrane decolorized 93.47% of the dye for the first 1 mL of solution filtered with a maximum adsorption capacity of 56.74 mg/g (mass of MB per 1 g of the cellulose nanofibers). But at the pH of 10, there is a rapid decolorization of the dye with a removal efficiency of 99.22% for 1 mL of feed solution filtered (<20 s) and a higher maximum adsorption capacity of 80.57 mg/g. In comparison, the maximum adsorption capacity reported for polyvinyl chloride mesoporous membranes is 75.9 mg/g and only 0.11 mg/g for the microcrystalline cellulose.[14,38] The enhanced decolorization at high pH is obviously

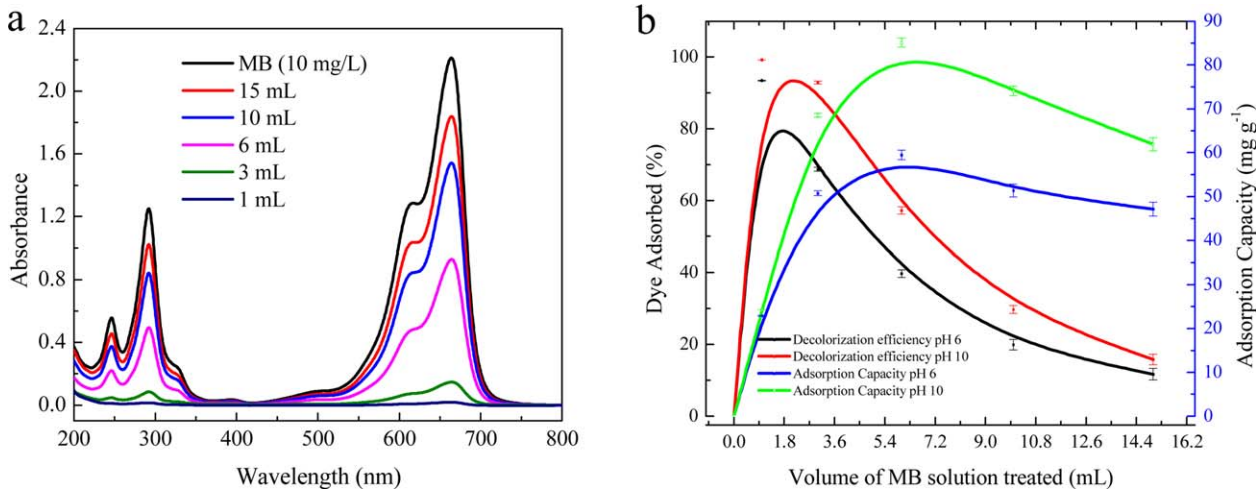


**Figure 10.** Decolorization of methylene blue using cellulose nanofibrous separation membranes: (**a**) UV–vis spectra of the feed and the permeate, for the membrane prepared from 15 mL of nanofibers dispersion at pH 10. (**b**) The dependence of the decolorization efficiency and adsorption capacity on the volume of a 10 mg/L MB solution for the membrane prepared from 15 mL of nanofibers dispersion at 30 °C. [Color figure can be viewed in the online issue, which is available at wileyonlinelibrary.com.]

ascribed to the reactive surface area of the fabricated membranes as demonstrated by Figure 10(a) and Supporting Information Figure S4, ASI. Meanwhile Cellulose nanofibers prepared by Wang *et al.* (2014) could only achieve a maximum decolorization efficiency of 35% after 60 s at similar pH, whereas the commercially available nanosized manganese oxide is only 16% efficient.[39]

Furthermore, for a given volume of the dye solution filtered the decolorization of the MB increases with the volume of nanofibers dispersion used in the membrane fabrication (i.e., thickness of the membrane). As shown in Figure 11, for membranes prepared from 5 to 20 mL of nanofibers dispersion at pH 6, the dye decolorized only increases from about 59 to 70%. Correspondingly the dye decolorized increased from about 92 to 96% for the membranes fabricated from nanofibers dispersion at pH 10. The reduced membrane porosity brought about by the nature of the cellulose nanofibers and the high affinity exhibited by membrane toward the neutral molecules is responsible for the adsorption of the MB through solution diffusion across the membranes. To this end, we have demonstrated that the arrangement of 1D and 2D polymer nanofibers dispersions by direct filtration to form nanoporous membranes represents a more efficient way of utilizing cellulose nanofibers. As UF eliminates the extreme sensitivity of conventional plant treatment steps of coagulation, sedimentation, and filtration to variable influent turbidities and particle charges, this contribution highlights the potential for the as fabricated membranes for the water treatment.

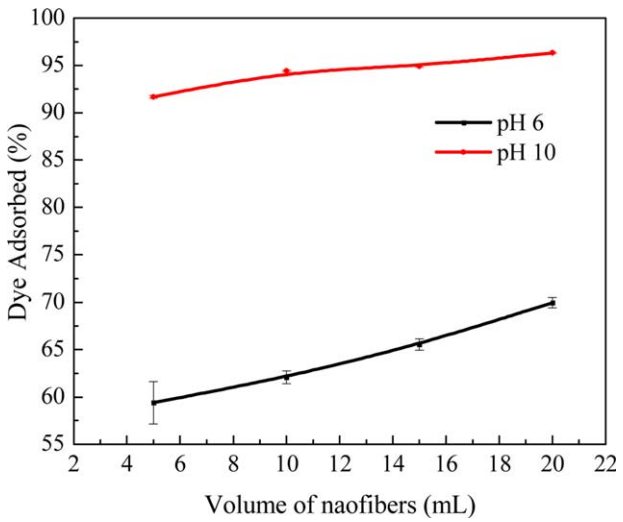


**Figure 11.** The dependence of the dye adsorbed on the volume of the cellulose nanofibers dispersion at different pH. [Color figure can be viewed in the online issue, which is available at wileyonlinelibrary.com.]

This facile fabrication route employed here is ecofriendly, as there is no hazardous chemical usage. And with no any such complex engineering controls involved except for the precise regulation of the physical parameters, it makes it highly favorable in comparison to conventional methods involving the use of toxic organic polymer solutions. Additionally, the use of the renewable and biodegradable cellulose material component would lower the overall cost of generating such membranes. These membranes can easily be reproduced and used in several filtration applications like laboratory water filtrations, cationic dye adsorbents, and protein concentration.

## CONCLUSIONS

Cellulose nanofibers with good thermal stability were prepared from commercial α-cellulose utilizing a green, simple and powerful HIUS mechanical method accompanied by mild pre-chemical treatments. Morphological observation confirms the successfully obtainment of nanofibers with an average diameter of 20 nm. An optimized alkaline concentration of 5 wt % was found to be appropriate as it increased the yield and boosted fiber crystallinity from 62% of original α-cellulose to 75% of the resultant nanofibers. A mild pre-chemical treatment is therefore essential to obtain purified and enhanced crystallinity

of the cellulose nanofibers. The as-prepared cellulose nanofibers form a nanoporous and hydrophilic barrier layer covering on a microporous support membrane producing high water flux nanofibrous UF membranes. Specifically, the 512 nm-thick membranes has ferritin and 10-nm gold nanoparticle rejections of 93.0 and 92.8% respectively and a pure water flux of $2.08 \times 10^3$ L/m$^2$/h/bar that is much higher than for most commercial filters. With an effective pore size of below 10 nm and a reactive surface area, the membranes have the capability of rapidly decolorizing methylene blue from its aqueous solutions with an adsorption capacity of 80.57 mg/g. Further modification of these composite supports forming a nanoporous structure with an extensive interconnected network of fine nanofibers presents a good direction for the development of cost effective separation and purification membranes.

## ACKNOWLEDGMENTS

The research was supported by National Nature Science Foundation of China Grant (No. 21306155), National Nature Science Foundation of Fujian Province of China Grant (No. 2014J05018) and the research fund for the Doctoral Program of Higher Education (No. 20120121120013).

## REFERENCES

1. Moon, R. J.; Martini, A.; Nairn, J.; Simonsen, J.; Youngblood, J. *Chem. Soc. Rev* **2011**, *40*, 3941.
2. Boufi, S. In Handbook of Biomass and Bioenergy Applications; Khalid, R. H.; Mohammad, J.; Umer, R., Eds.; Springer: Switzerland, **2014**; Chapter 1, p 267.
3. Abdul Khalil, H. P. S.; Bhat, A. H.; Ireana Yusra, A. F. *Carbohydr. Polym.* **2012**, *87*, 963.
4. Koga, H.; Nogi, M.; Komoda, N.; Nge, T. T.; Sugahara, T.; Suganuma, K. *NPG Asia Mater.* **2014**, *6*, e93.
5. Turbak, A. F.; Snyder, F. W.; Sandberg, K. R. *J. Appl. Polym. Sci. Symp.* **1983**, *37*, 815.
6. Siró, I.; Plackett, D. *Cellulose* **2010**, *17*, 459.
7. Lau, W. J.; Ismail, A. F.; Misdan, N.; Kassim, M. A. *Desalination* **2012**, *28*, 190.
8. Kulpinski, P. *J. Appl. Polym. Sci.* **2005**, *98*, 1855.
9. Andrè, P.; Kenneth, N. M.; Shusheng, P.; Staiger, M. P. *Chem. Rev.* **2009**, *109*, 6712.
10. Varanasi, S.; Low, Z. X.; Batchelor, W. *Chem. Eng. J.* **2015**, *265*, 138.
11. Ma, H. Y.; Burger, C.; Hsiao, B. S.; Chu, B. *J. Membr. Sci.* **2014**, *454*, 272.
12. Brinchi, L.; Cotana, F.; Fortunati, V.; Kenny, J. M. *Carbohydr. Polym.* **2013**, *94*, 154.
13. Zhao, H. P.; Feng, X. Q.; Gao, H. *J. Appl. Phys. Lett.* **2007**, *90*, 073112.
14. Wang, S.; Cheng, Q. *J. Appl. Polym. Sci.* **2009**, *113*, 1270.
15. Bang, J. H.; Suslick, K. S. *Adv. Mater.* **2010**, *22*, 1039.
16. Chen, W. S.; Yu, H. P.; Liu, Y. X.; Chen, P.; Zhang, M. X.; Hai, Y. F. *Carbohydr. Polym.* **2011**, *83*, 1804.
17. Nasri-Nasrabadi, B.; Behzad, T.; Bagheri, R. *J. Appl. Polym. Sci.* **2014**, *131*, 40063.
18. Silvério, H. A.; Flauzino Neto, W. P.; Dantas, N. O.; Pasquini, D. *Ind. Crop. Prod.* **2013**, *44*, 427.
19. Chen, W.; Yu, H.; Liu, Y. *Carbohydr. Polym.* **2011**, *86*, 453.
20. Morán, J. I.; Alvarez, V. A.; Cyras, V. P.; Vázquez, A. *Cellulose* **2007**, *15*, 149.
21. Tischer, P. C. S. F.; Sierakowski, M. R.; Westfahl, H.; Tischer, C. A. *Biomacromolecules* **2010**, *11*, 1217.
22. Szczęsna-Antczak, M.; Kazimierczak, J.; Antczak, T. *Fibres Text. East Eur.* **2012**, *20*, 8.
23. Huber, T.; Jörg, M. S.; Curnow, O.; Shusheng, P.; Bickerton, S.; Staiger, M. P. *J. Mater. Sci.* **2012**, *47*, 1171.
24. Ke, Z.; Zhang, Q. G.; Li, H. M.; Guo, N. N.; Zhu, A. M.; Liu, Q. L. *Nanoscale* **2014**, *6*, 10363.
25. Segal, L.; Creely, J. J.; Martin, A. E., Jr.; Conrad, C. M. *Text. Res. J.* **1959**, 786.
26. Faizal, S.; Zhang, Q. G.; Chao, D.; Yi, G.; Zhu, A. M.; Liu, Q. L. *J. Membr. Sci.* **2014**, *454*, 339.
27. Chan, C. H.; Chia, C. H.; Zakaria, S.; Sajab, M. S.; Chin, S. X. *RSC Adv.* **2015**, *5*, 18204.
28. Guo, N. N.; Zhang, Q. G.; Li, H. M.; Wu, X. M.; Liu, Q. L.; Zhu, A. M. *Ind. Eng. Chem. Res.* **2014**, *53*, 20068.
29. Chen, W.; Yu, H.; Liu, Y.; Hai, Y.; Zhang, M.; Chen, P. *Cellulose* **2011**, *18*, 433.
30. Gwon, J. G.; Lee, S. Y.; Doh, G. H.; Kim, J. H. *J. Appl. Polym. Sci.* **2010**, *116*, 3212.
31. Dinand, E.; Vignon, M.; Chanzy, H.; Heux, L. *Cellulose* **2002**, *9*, 7.
32. Tarbuk, A.; Grancaric, A.; Leskovac, M. *Cellulose* **2014**, *21*, 2167.
33. Oh, S. Y.; Yoo, D. I.; Shin, Y. S.; Seo, G. *Carbohydr. Res.* **2005**, *340*, 417.
34. Zhang, Q.; Ghosh, S.; Samitsu, S.; Peng, X.; Ichinose, I. *J. Mater. Chem.* **2011**, *21*, 1684.
35. Ding, Y. X.; Sui, Y. C.; Tai-Shung, C. *Chem. Eng. Sci.* **2013**, *87*, 194.
36. Elizabeth, A.; Aviv, D.; Vitaly, G. *J. Membr. Sci.* **2012**, *394*, 89.
37. Tao, M.; Xue, L. X.; Liu, F.; Jiang, L. *Adv. Mater.* **2014**, *26*, 2943.
38. Bouhdadi, R.; Benhadi, S.; Molina, S.; George, B.; El Moussaouiti, M.; Merlin, A. *Maderas: Cienc. Tecnol.* **2011**, *13*, 105.
39. Wang, Y.; Zhang, X. F.; He, X.; Zhang, W.; Zhang, X. X.; Lu, C. H. *Carbohydr. Polym.* **2014**, *110*, 302.